Lie symmetry group theory for turbulence modelling and simulation

Aziz Hamdouni*, Dina Razafindralandy*, Marx Chhay†, and Nazir Al Sayed‡
*Laboratoire des Sciences de l'Ingénieur pour l'Environnement – UMR 7356
Université de La Rochelle – France
†Laboratoire Optimisation de la Conception et Ingénieurie de l'Environnement – UMR 5271
Université de Savoie – France
‡Laboratoire de Mécanique des Structures Industrielles Durables – UMR EDF/CNRS/CEA 8193
EDF R&D – France

***Abstract*—In this paper, we present some applications of the Lie-group theory to fluid mechanics problems. We present how to use the Lie-group theory to deduce conservation laws of the Navier-Stokes equations and scaling laws of turbulent flows. We also develop symmetry preserving turbulent models, and show how the symmetry theory can contribute to build robust numerical schemes.**

I. Introduction

The literature shows that the Lie-symmetry group theory constitutes a powerful modelling tool in engineering science. They allow, for instance, the computation of Green function of linear equations. In addition, symmetries are extensively used in literature to compute self-similar solutions of various equations. In turbulence, vortex solutions of the Navier-Stokes equations was found as special self-similar solutions. Finally, we mention that the symmetries may give an information on the large-time behaviour of the solution. To some extent, the symmetries traduce the physics of the equations.

In this communication, we present some applications to fluid mechanics, and especially to the modelling and simulation of turbulent flows. In SECTION II, we recall briefly the theory of Lie-symmetry group and how to compute them. We then list the Lie-symmetry transformations of the Navier-Stokes equations in the non-isothermal case. Next, we recall the Nœther's theorem which links the symmetries of an equation to conservation laws in the case of a Lagrangian-described system. We then show how to extend this theorem to non-Lagrangian systems and how to find conservation laws of the Navier-Stokes equations.

In SECTION IV, we are especially interested in turbulent flows. We use the Lie-group theory to find wall and scaling laws of non-isothermal turbulent flows. Next, we develop symmetry preserving turbulence models and show their numerical performance.

In SECTION V, we build robust numerical schemes, based on symmetry preservation.

II. Lie symmetry group theory and application to the non-isothermal Navier-Stokes equations

Instead of presenting the Lie symmetry group theory on a general equation, we apply it directly to the non-isothermal Navier-Stokes equations:

$$\begin{cases} \dfrac{\partial \boldsymbol{u}}{\partial t} + \operatorname{div}(\boldsymbol{u}\otimes\boldsymbol{u}) + \dfrac{1}{\rho}\nabla p - \nu\Delta\boldsymbol{u} - \beta g\theta\,\boldsymbol{e}_3 = 0 \\ \dfrac{\partial \theta}{\partial t} + \operatorname{div}(\theta\boldsymbol{u}) - \Delta\theta = 0 \\ \operatorname{div}\,\boldsymbol{u} = 0 \end{cases} \tag{1}$$

A continuous symmetry of equations (1) is a transformation

$$T_\epsilon : \quad \boldsymbol{q} = (t, \boldsymbol{x}, \boldsymbol{u}, p, \theta) \longmapsto \hat{\boldsymbol{q}} = (\hat{t}, \hat{\boldsymbol{x}}, \hat{\boldsymbol{u}}, \hat{p}, \hat{\theta}), \tag{2}$$

depending smoothly on the parameter ϵ, and which leave the set of solutions of (1) invariant. In other words, T_ϵ is a symmetry of (1) if

$$\boldsymbol{NS}(\boldsymbol{q}) = \boldsymbol{0} \quad \Longrightarrow \quad \boldsymbol{NS}(\hat{\boldsymbol{q}}) = \boldsymbol{0} \tag{3}$$

where $\boldsymbol{NS}$ designate equations (1). A Lie symmetry group of $\boldsymbol{NS}$ is a set of continuous transformations which has a Lie group structure.

Definition (3) permits to compute some but not all symmetry groups of $\boldsymbol{NS}$. In order to be exhaustive, one introduces the tangent vector:

$$\boldsymbol{X} = \xi_t \frac{\partial}{\partial t} + \xi_{\boldsymbol{x}} \cdot \frac{\partial}{\partial \boldsymbol{x}} + \xi_{\boldsymbol{u}} \cdot \frac{\partial}{\partial \boldsymbol{u}} + \xi_p \frac{\partial}{\partial p} + \xi_\theta \frac{\partial}{\partial \theta} \tag{4}$$

where

$$\xi_q = \left.\frac{\partial \hat{q}}{\partial \epsilon}\right|_{\epsilon=0}. \tag{5}$$

A tangent vector of a Lie group is also called its generator since, knowing the components ξ_q of $\boldsymbol{X}$, one can determine the elements T_ϵ of the group by solving the equation

$$\frac{\mathrm{d}\hat{\boldsymbol{q}}}{\mathrm{d}\epsilon} = \xi(\hat{\boldsymbol{q}}), \quad \hat{\boldsymbol{q}}(\epsilon = 0) = \boldsymbol{q}. \tag{6}$$

Definition (3) is equivalent to the infinitesimal condition

$$\boldsymbol{NS}(\boldsymbol{q}) = 0 \quad \Longrightarrow \quad \boldsymbol{X}^{(2)} \cdot \boldsymbol{NS}(\boldsymbol{q}) = 0. \tag{7}$$

$\boldsymbol{X}^{(2)}$ is a prolongation of $\boldsymbol{X}$ which accounts for the first and second order partial derivatives in the equations (see [1]–[3]). This condition enables to compute the tangent vectors of all the Lie symmetry groups of (1):

$$\boldsymbol{X}_1 \;=\; \frac{\partial}{\partial t} \tag{8}$$

$$\boldsymbol{X}_2 \;=\; \zeta(t)\frac{\partial}{\partial p} \tag{9}$$

$$\boldsymbol{X}_3 \;=\; \beta g\, x_3 \frac{\partial}{\partial p} + \frac{1}{\rho}\frac{\partial}{\partial \theta} \tag{10}$$

$$\boldsymbol{X}_4 \;=\; x_2\frac{\partial}{\partial x_1} - x_1\frac{\partial}{\partial x_2} + u_2\frac{\partial}{\partial u_1} - u_1\frac{\partial}{\partial u_2} \tag{11}$$

$$\boldsymbol{X}_{4+i} \;=\; \alpha_i(t)\frac{\partial}{\partial x_i} + \dot\alpha_i(t)\frac{\partial}{\partial u_i} - \rho\, x_i\ddot\alpha_i(t)\frac{\partial}{\partial p}, \quad i = 1,2,3, \tag{12}$$

$$\boldsymbol{X}_8 \;=\; 2t\frac{\partial}{\partial t} + \boldsymbol{x}\cdot\frac{\partial}{\partial \boldsymbol{x}} - \boldsymbol{u}\cdot\frac{\partial}{\partial \boldsymbol{u}} - 2p\frac{\partial}{\partial p} - 3\theta\frac{\partial}{\partial \theta} \tag{13}$$

where ζ and the α_i's are arbitrary functions of time. The dot symbol ($\dot{}$) stands for time derivation.

We can also consider symmetries (which are sometimes called equivalence transformations) of the form

$$(t, \boldsymbol{x}, \boldsymbol{u}, p, \theta, \nu, \kappa) \;\longmapsto\; (\hat t, \hat{\boldsymbol{x}}, \hat{\boldsymbol{u}}, \hat p, \hat\theta, \hat\nu, \hat\kappa). \tag{14}$$

Such symmetries take a solution of (1) into a solution of other non-isothermal Navier–Stokes equations with different values of ν and κ. Applying condition (7) leads to the infinitesimal generator

$$\boldsymbol{X}_9 = \boldsymbol{x}\cdot\frac{\partial}{\partial \boldsymbol{x}} + \boldsymbol{u}\cdot\frac{\partial}{\partial \boldsymbol{u}} + 2p\frac{\partial}{\partial p} + \theta\frac{\partial}{\partial \theta} + 2\nu\frac{\partial}{\partial \nu} + 2\kappa\frac{\partial}{\partial \kappa}. \tag{15}$$

From these generators, the symmetry group of (1) can be identified. They are, respectively:

- the group of *time translations*:

$$(t, \boldsymbol{x}, \boldsymbol{u}, p, \theta) \;\longmapsto\; (t+\epsilon, \boldsymbol{x}, \boldsymbol{u}, p, \theta), \tag{16}$$

- the group of *pressure translations*:

$$(t, \boldsymbol{x}, \boldsymbol{u}, p, \theta) \;\longmapsto\; (t, \boldsymbol{x}, \boldsymbol{u}, p+\zeta(t), \theta), \tag{17}$$

- the group of *pressure-temperature translations*:

$$(t, \boldsymbol{x}, \boldsymbol{u}, p, \theta) \;\longmapsto\; (t, \boldsymbol{x}, \boldsymbol{u}, p+\epsilon\,\beta g\, x_3, \theta + a/\rho), \tag{18}$$

- the group of *horizontal rotations*:

$$(t, \boldsymbol{x}, \boldsymbol{u}, p, \theta) \;\longmapsto\; (t, \mathsf{R}\boldsymbol{x}, \mathsf{R}\boldsymbol{u}, p, \theta) \tag{19}$$

  where R is a 2D (constant) rotation matrix,
- the three-parameter group of *generalized Galilean transformations*:

$$(t, \boldsymbol{x}, \boldsymbol{u}, p, \theta) \;\longmapsto\; (t, \boldsymbol{x}+\boldsymbol{\alpha}(t), \boldsymbol{u}+\dot{\boldsymbol{\alpha}}(t), p+\rho\,\boldsymbol{x}\cdot\ddot{\boldsymbol{\alpha}}(t), \theta), \tag{20}$$

- the group of the *first scaling transformations*:

$$(t, \boldsymbol{x}, \boldsymbol{u}, p, \theta) \longmapsto (\mathrm{e}^{2\epsilon}\, t, \mathrm{e}^{\epsilon}\, \boldsymbol{x}, \mathrm{e}^{-\epsilon}\, \boldsymbol{u}, \mathrm{e}^{-2\epsilon}\, p, \mathrm{e}^{-3\epsilon}\, \theta) \tag{21}$$

  which shows how $\boldsymbol{u}$, p and θ change when the spatio-temporal scale is multiplied by $(\mathrm{e}^{\epsilon}, \mathrm{e}^{2\epsilon})$,
- and the group of the *second scaling transformations*:

$$(t, \boldsymbol{x}, \boldsymbol{u}, p, \theta, \nu, \kappa) \mapsto (t, \mathrm{e}^{\epsilon}\, \boldsymbol{x}, \mathrm{e}^{\epsilon}\, \boldsymbol{u}, \mathrm{e}^{2\epsilon} p, \mathrm{e}^{\epsilon}\, \theta, \mathrm{e}^{2\epsilon}\nu, \mathrm{e}^{2\epsilon}\kappa) \tag{22}$$

  which shows the consequence of a modification of the spatial scale.

Equations (1) own other known non-Lie symmetries, which are:

- the *reflections* about x_1 and x_2 axes
- and the *material indifference* in the limit of a 2D horizontal flow in a simply connected domain [4]:

$$(t, \boldsymbol{x}, \boldsymbol{u}, p) \mapsto (t\ ,\ \mathsf{R}(t)\hat{\boldsymbol{x}}\ ,\ \mathsf{R}(t)\boldsymbol{u} + \dot{\mathsf{R}}(t)\boldsymbol{x}\ ,\ \hat p) \tag{23}$$

  with

$$\hat p = p - 3\omega\phi + \omega^2\|\boldsymbol{x}\|^2/2$$

  where $\mathsf{R}(t)$ is an horizontal 2D rotation matrix with angle ωt, ω a real parameter, and ϕ the usual 2D stream function.

In the next section, we recall Nœther's theorem which links symmetries to conservation laws.

III. Symmetry and conservation laws

Consider a system described by a Lagrangian action

$$\mathcal{L}[\boldsymbol{w}] = \int_\Omega L(\boldsymbol{y}, \boldsymbol{w}, \dot{\boldsymbol{w}}) \tag{24}$$

and the corresponding Euler-Lagrange equation

$$\frac{\partial L}{\partial \boldsymbol{w}} - \mathrm{Div}\,\frac{\partial L}{\partial \dot{\boldsymbol{w}}} = 0, \tag{25}$$

where $\mathrm{Div}\, f = \sum_i \dfrac{\partial f}{\partial y_i}$ for any smooth function f.

Nœther showed that to each Lie group which leaves the action $\mathcal{L}$ invariant corresponds a conservation law [5]. More precisely, if

$$\boldsymbol{X}\cdot\mathcal{L} = 0 \tag{26}$$

then

$$\mathrm{Div}\,\boldsymbol{C} = 0. \tag{27}$$

The conserved quantity $\boldsymbol{C}$ is defined by

$$\boldsymbol{C} = L\xi_{\boldsymbol{y}} + \left[\frac{\partial L}{\partial \gamma}\right]^T (\xi_{\boldsymbol{w}} - \gamma\xi_{\boldsymbol{y}}) \tag{28}$$

where $\gamma_k^j = \dfrac{\partial w_j}{\partial y_k}$.

Unfortunately, Nœther's theorem does not apply directly to equations (1) for these later do not have a Lagrangian structure. However, one can associate to (1) adjoint equations such that, together, they derive from

a "Bilagrangian" function. Indeed, consider, for example, the isothermal case. Then, the Navier-Stokes equations

$$\begin{cases} \dfrac{\partial \boldsymbol{u}}{\partial t} + \boldsymbol{u}\cdot\nabla\boldsymbol{u} + \dfrac{1}{\rho}\nabla p - \nu\Delta\boldsymbol{u} = 0 \\ \\ \text{div } \boldsymbol{u} = 0 \end{cases} \tag{29}$$

and their adjoint equations

$$\begin{cases} -\dfrac{\partial \boldsymbol{v}}{\partial t} + \boldsymbol{v}\cdot\nabla\boldsymbol{u} - \boldsymbol{u}\cdot\nabla v - \dfrac{1}{\rho}\nabla s - \nu\Delta\boldsymbol{v} = 0 \\ \\ \text{div } \boldsymbol{u} = 0 \end{cases} \tag{30}$$

derive from the Bilagrangian

$$\begin{aligned} L = \frac{1}{2}\left(\frac{\mathrm{d}\boldsymbol{u}}{\mathrm{d}t}\cdot\boldsymbol{v} - \boldsymbol{u}\cdot\frac{\mathrm{d}\boldsymbol{v}}{\mathrm{d}t}\right) + \left(\frac{1}{\rho}s - \frac{1}{2}\boldsymbol{u}\cdot\boldsymbol{v}\right)\text{div}\,\boldsymbol{u} \\ - \frac{1}{\rho}p\,\text{div}\,\boldsymbol{v} + \nu\,\text{tr}(\nabla\boldsymbol{u}^T\nabla v). \end{aligned} \tag{31}$$

In these expressions, $\boldsymbol{v}$ and s are adjoint variables. With this extension of the notion of Lagrangian system, Nœther's theorem can be applied to the Navier-Stokes equations to find conservation laws.

In the next section, we show some applications of symmetry analysis to the understanding and simulation of turbulence.

IV. Symmetry and turbulence

In the first subsection, we present the derivation of scaling laws of turbulent flows from symmetry. Then we show how to build symmetry-preserving turbulence models.

A. Scaling laws of non-isothermal fluid flows

Consider a turbulent channel fluid flow. We decompose the velocity, pressure and temperature into mean and fluctuating parts such that the mean parts depend only on x_2 (wall normal coordinate):

$$\begin{aligned} &\boldsymbol{u} = \boldsymbol{u}' + \boldsymbol{U}(x_2), \\ &p = p' + P(x_2) - Kx_1, \\ &\theta = \theta' + \Theta(x_2) \end{aligned} \tag{32}$$

K is a consatant pressure gradient in streamwise direction. We assume that the mean flow is parallel to the walls. The equations of the fluctuating quantities are then:

$$\begin{cases} \dfrac{\partial u_i'}{\partial t} + U_1\dfrac{\partial u_i'}{\partial x_1} + u_2'\dfrac{\mathrm{d}U_1}{\mathrm{d}x_2}\delta_{i1} - \left(K + \nu\dfrac{\partial^2 U_1}{\partial x_2^2}\right)\delta_{i1} + \\ \left(\dfrac{\partial P}{\partial x_2} - \beta g\Theta\right)\delta_{i2} + \dfrac{\partial u_i'u_k'}{\partial x_k} + \dfrac{\partial p'}{\partial x_i} - \nu\dfrac{\partial^2 u_i'}{\partial x_k^2} - \beta g\theta'\delta_{i2} = 0 \\ \\ \dfrac{\partial \theta'}{\partial t} + \dfrac{\partial \theta' u_j'}{\partial x_j} - \kappa\dfrac{\partial^2\theta'}{\partial x_j^2} - \kappa\dfrac{\partial^2\Theta}{\partial x_2^2} + u_2'\dfrac{\partial\Theta}{\partial x_2} + U_1\dfrac{\partial\theta'}{\partial x_1} = 0 \\ \\ \dfrac{\partial u_k'}{\partial x_k} = 0. \end{cases} \tag{33}$$

Using the described theory, one can compute the Lie symmetry groups of (33) which, for lack of space, are not listed here but can be found in [6].

A scaling law of equations (33) verifies the condition

$$\boldsymbol{X}\cdot U_1 = 0, \quad \boldsymbol{X}\cdot\Theta = 0 \tag{34}$$

where $\boldsymbol{X}$ is the generator of one of the Lie symmetry groups of (33). Solving these equations leads to the following scaling laws (among others).

- The linear law which can be found in the middle region of a Couette flow and in the viscous sublayer of a boundary flow:

$$U_1 = C_1x_2 + C_3, \quad \Theta = C_2x_2 + C_4. \tag{35}$$

- The classical logarithmic wall law and its corresponding temperature law:

$$U_1 = C_1\ln(x_2{+}b){+}C_3, \quad \Theta = C_2[x_2{+}b]^{-1}{+}C_4. \tag{36}$$

- The exponential law:

$$U_1 = C_1\exp(Cx_2) + C_3, \quad \Theta = C_2\exp(2Cx_2) + C_4. \tag{37}$$

- The power law of velocity discovered by Oberlack [7] in the buffer region of a boundary layer and its temperature counterpart:

$$U_1 = C_1(x_2+b)^a + C_3, \quad \Theta = C_2(x_2+b)^{2a-1} + C_4. \tag{38}$$

As we now know, symmetries contain fundamental physical properties, such as conservation laws and wall laws. It is then essential not to destroy them when developing a model whether it be a theoretical or a numerical one. In the next subsection, we present symmetry-preserving models for non-isothermal fluid flows, and, after that, we show how to develop a symmetry-preserving numerical models.

B. Turbulence modelling

A direct simulation of a fluid flow would cost too much because it requires a very fine grid. Hence, instead of solving equations (1), we consider the large-eddy simulation approach [8] which consists in computing an (filtered) approximation $(\overline{\boldsymbol{u}}, \overline{p}, \overline{\theta})$ of $(\boldsymbol{u}, p, \theta)$. It verifies the equations

$$\begin{cases} \dfrac{\partial\overline{\boldsymbol{u}}}{\partial t} + \text{div}(\overline{\boldsymbol{u}}\otimes\overline{\boldsymbol{u}}) + \dfrac{1}{\rho}\nabla\overline{p} - \text{div}(\overline{\tau} - \tau_s) - \beta g\overline{\theta}\,\boldsymbol{e}_3 = 0 \\ \\ \dfrac{\partial\overline{\theta}}{\partial t} + \text{div}(\overline{\theta}\overline{\boldsymbol{u}}) - \text{div}(\overline{\mathbf{h}} - \mathbf{h}_s) = 0 \\ \\ \text{div}\,\overline{\boldsymbol{u}} = 0. \end{cases} \tag{39}$$

In these equations, $\tau = 2\nu\mathsf{S}$ and $\tau_s = \overline{\boldsymbol{u}\otimes\boldsymbol{u}} - \overline{\boldsymbol{u}}\otimes\overline{\boldsymbol{u}}$ are respectively the molecular and the subgrid stress tensors, whereas $\mathbf{h} = \kappa\nabla\theta$ and $\mathbf{h}_s = \overline{\theta\boldsymbol{u}} - \overline{\theta}\overline{\boldsymbol{u}}$ are molecular and the subgrid heat fluxes. τ_s and $\mathbf{h}_s$ have to be modelled.

Many models have been proposed in the literature but most of them destroy the symmetry properties of equations (1) [9]. So, we propose new ones using the symmetry approach.

It is clear that time translations (16), applied to $(t, \boldsymbol{x}, \overline{\boldsymbol{u}}, \overline{p}, \overline{\theta})$, are symmetries of the filtered equations (39) if τ_s and $\mathbf{h}_s$ do not explicitly depend on t. It is also straightforward to check that the pressure-temperature translations, and the Galilean transformations remain symmetries of (39) if τ_s and $\mathbf{h}_s$ depend only on $\overline{S}$ and $\overline{\mathbb{T}} = \nabla\overline{\theta}$. From the classical theory of isotropic functions and the invariance under scale symmetries, we deduce a class of symmetry preserving models

$$\begin{cases} -\tau_s^d = \nu F_1 \overline{S} + \nu F_2 \frac{\mathrm{Adj}^d \overline{S}}{||\overline{S}||} + \nu F_3 \frac{(\overline{\mathbb{T}}\otimes\overline{\mathbb{T}})^d}{||\overline{S}||^3} \\ \qquad + \nu F_4 \frac{[\overline{S}(\overline{\mathbb{T}}\otimes\overline{\mathbb{T}})]^d}{||\overline{S}||^4} + \nu F_5 \frac{\overline{S}[(\overline{\mathbb{T}}\otimes\overline{\mathbb{T}})\overline{S}]^d}{||S||^5}, \\ -\mathbf{h}_s = \kappa \left(F_6 + F_7 \frac{\overline{S}}{||\overline{S}||} + F_8 \frac{\overline{S}^2}{||\overline{S}||^2} \right) \overline{\mathbb{T}}. \end{cases} \tag{40}$$

The F_i are arbitrary functions of the invariant quantities

$$v = \frac{\det \overline{S}}{||\overline{S}||^3}, \quad \frac{\overline{\mathbb{T}}^2}{||\overline{S}||^4}, \quad \frac{\overline{\mathbb{T}} \cdot \overline{S\mathbb{T}}}{||\overline{S}||^5}, \quad \frac{\overline{S\mathbb{T}} \cdot \overline{S\mathbb{T}}}{||\overline{S}||^6} \tag{41}$$

which naturally arise from the symmetry requirements. Superscript $(^d)$ symbolizes the deviatoric operator and $\mathrm{Adj}\,\overline{S}$ the adjugate of $\overline{S}$.

Many simpler models may be deduced from (40). One of them which vanishes at walls with a rate $O(x_2^3)$ (if x_2 is the wall normal coordinate) is the following:

$$\begin{cases} -\tau_s^d = C_m \nu \left[\left(2 - 2\,\mathrm{e}^{-v^3} - 9v^3\mathrm{e}^{-v^3}\right)\overline{S} + 3v^2\mathrm{e}^{-v^3} \frac{\mathrm{Adj}^d \overline{S}}{||\overline{S}||} \right] \\ -\mathbf{h}_s = C_t \kappa (1 - \mathrm{e}^{-v^3}) \overline{\mathbb{T}}. \end{cases} \tag{42}$$

A numerical test on model (42) is presented in the next subsection.

C. Numerical test

Consider an air flow in the ventilated room presented in figure 1 [10]. The dimension of the room is 1.04m×1.04m×0.7m. The inlet and outlet heights are respectively 0.018 and 0.024m, and the inlet velocity is 0.57m/s. The floor is heated at 35°C while the other walls are maintained at 15°C. The Reynolds number, based on the inlet height and the inlet velocity, is 678. Figure 2, left, shows that the horizontal velocity given by the invariant model (42) fits very well the experimental data. The concordance is particularly striking near the walls. The maximum values near the floor and near the ceilor are correctly predicted. This good agreement can be explained by the non-violation of the wall laws by the invariant model. Almost everywhere, the invariant model provides better results than the classical Smagorinsky

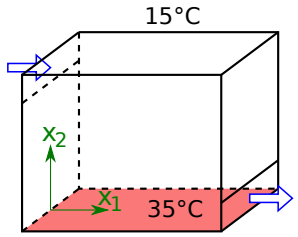

Fig. 1. Geometry of the room

model [11] which seems very dissipative. The vertical velocity presents the same trend. Figures 3 report the

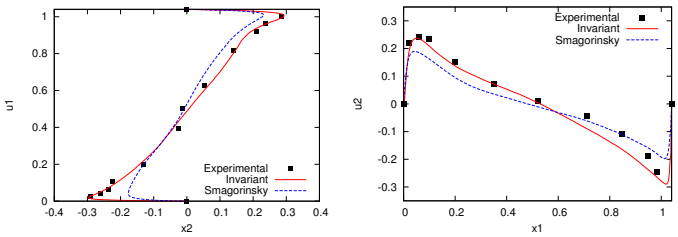

Fig. 2. Horizontal (left) and vertical (right) mean velocity profile at respectively $x_1 = 0.501$m and $x_2 = 0.501$m, at the half-width

temperature profiles along a vertical and an horizontal lines, passing through the middle of the room. It can be observed on these figures that the invariant model predicts the temperature behavior better than the Smagorinsky model does. However, both models under-estimate the experimental measurements. This may not due to the models but to the (well-known) bad control of boundary conditions during the experimentation. Indeed, some phenomena such as radiation or the variation of temperature at the wall are hard to take into account.

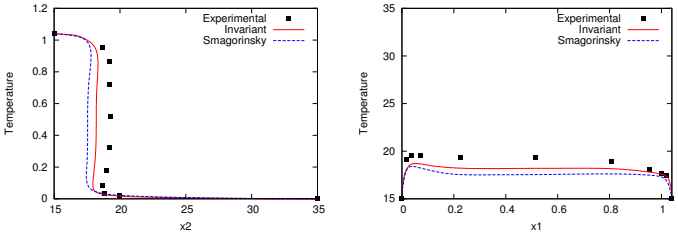

Fig. 3. Mean temperature profiles at $x_1 = 0.501$m (left) and at $x_2 = 0.501$m (right), at the half-width

In the last section, we present how to preserve the symmetry group of an equation at the discrete scale.

V. Symmetry-based numerical schemes

Consider a differential equation

$$E(\boldsymbol{x}, \boldsymbol{u}) = 0 \tag{43}$$

on a domain Ω. The latter is discretized into discrete points $\underline{\boldsymbol{x}} = (\boldsymbol{x}_1, ..., \boldsymbol{x}_J)$ verifying a relation

$$\Phi(\underline{\boldsymbol{x}}) = 0. \tag{44}$$

Φ is called the mesh. Similarly, $\boldsymbol{u}$ is discretized into a sequence $\underline{\boldsymbol{u}} = (\boldsymbol{u}_1, ..., \boldsymbol{u}_J)$. We denote $\boldsymbol{z}_j = (\boldsymbol{x}_j, \boldsymbol{u}_j)$ and $\boldsymbol{z} = (\boldsymbol{z}_1, ..., \boldsymbol{z}_J)$.

A discretization scheme of equation (43), with an accuracy order $(q_1, ..., q_M)$, is a couple of functions (N, Φ) such that

$$N(\boldsymbol{z}) = O\left((\Delta x^1)^{q_1}, ..., (\Delta x^M)^{q_M}\right) \quad (45)$$

$$\Phi(\boldsymbol{z}) = 0 \quad (46)$$

as soon as $\boldsymbol{u}_j = \boldsymbol{u}(\boldsymbol{x}_j)$ for all $j = 1, ..., J$. Δx^m is the step size in the m-th direction, $m = 1, ..., M$. Φ has been extended to $\boldsymbol{z}$ in (46) such that N and Φ has the same argument. This extension is also necessary when the mesh changes with the values of $\boldsymbol{u}$ (adaptative mesh, ...).

Starting from any usual scheme (N, Φ), it is possible, with the use of moving frame, to derive a new scheme $(\tilde{N}, \tilde{\Phi})$ which is invariant under the symmetry group of equation (43). The invariance of the scheme means:

$$\begin{cases} \widetilde{N}(\boldsymbol{z}) = 0 & \Rightarrow \quad \widetilde{N}(T(\boldsymbol{z})) = 0 \\ \widetilde{\Phi}(\boldsymbol{z}) = 0 & \Rightarrow \quad \widetilde{\Phi}(T(\boldsymbol{z})) = 0 \end{cases} \quad (47)$$

for any Lie symmetry T of the equation.

Indeed, let G be a multi-parameter group G acting regularly and freely on a manifold $\mathcal{M}$. A (right) moving frame is a map $\rho : \mathcal{M} \mapsto G$ verifying the equivariance condition [12], [13]:

$$\rho[T.\boldsymbol{y}] = \rho[\boldsymbol{y}]T^{-1}, \quad \forall \boldsymbol{y} \in \mathcal{M}, g \in G. \quad (48)$$

A fundamental theorem [12] then shows that when G is the symmetry group of the equation and ρ a moving frame then the scheme $(\tilde{N}, \tilde{\Phi})$ defined by

$$\tilde{N}(\boldsymbol{z}) = N(\rho[\boldsymbol{z}].\boldsymbol{z}), \quad \tilde{\Phi}(\boldsymbol{z}) = \Phi(\rho[\boldsymbol{z}].\boldsymbol{z}) \quad (49)$$

is an invariant numerical scheme of the same order for the same equation.

In what follows, we consider Burgers'equation

$$\frac{\partial u}{\partial t} + u\frac{\partial u}{\partial x} = \nu \frac{\partial^2 u}{\partial x^2}. \quad (50)$$

and we compare some classical schemes, namely the standard Euler FTCS, the Lax–Wendroff and the Crank–Nicholson schemes, to their invariant versions. The symmetry transformations of (50) are:

- time translations:

$$g_1 : (t, x, u) \longmapsto (t + \epsilon_1, x, u), \quad (51)$$

- space translations:

$$g_2 : (t, x, u) \longmapsto (t, x + \epsilon_2, u), \quad (52)$$

- scaling transformations:

$$g_3 : (t, x, u) \longmapsto (te^{2\epsilon_3}, xe^{\epsilon_3}, ue^{-\epsilon_3}), \quad (53)$$

- projections:

$$g_4 : (t, x, u) \longmapsto \left(\frac{t}{1-\epsilon_4 t}, \frac{x}{1-\epsilon_4 t}, (1-\epsilon_4 t)u + \epsilon_4 x\right), \quad (54)$$

- and Galilean boosts:

$$g_5 : (t, x, u) \longmapsto (t, x + \epsilon_5 t, u + \epsilon_5). \quad (55)$$

In practice, choosing a moving frame is equivalent to deciding the values of the parameters ϵ_i.

As an example, the described method yields the following invariant FTCS scheme [14], [15]:

$$\frac{[1-\epsilon_4(t^{n+1}+\epsilon_1)]u_j^{n+1} + \epsilon_4(x_j^{n+1}+\epsilon_2) - u_j^n}{t^{n+1}+\epsilon_1}[1-\epsilon_4(t^{n+1}+\epsilon_1)] + (u_j^n + \epsilon_5)\left[\frac{u_{j+1}^n - u_{j-1}^n}{2(x_{j+1}^n + \epsilon_2} + \epsilon_4\right] = \nu \frac{u_{j+1}^n - 2u_j^n + u_{j-1}^n}{(x_{j+1}^n + \epsilon_2)^2}. \quad (56)$$

The moving frame corresponds to

$$\begin{array}{l} \epsilon_1 = -t_j^n, \quad \epsilon_2 = -x_j^n, \quad \epsilon_4 = -\frac{u_{j+1}^n - u_{j-1}^n}{2\Delta x} \\ \epsilon_5 = du_{j+1}^n + eu_j^n + du_{j-1}^n \quad \text{with} \quad e + 2d = -1. \end{array} \quad (57)$$

In a first test, we solve numerically equation (50) on $\Omega = \{(t, x) \in [0, 1] \times [-2, 2]\}$ with the exact solution

$$u(t, x) = \frac{-\sinh(\frac{x}{2\nu})}{\cosh(\frac{x}{2\nu}) + \exp(-\frac{t}{4\nu})} \quad (58)$$

and $\nu = 5.10^{-3}$. The space step size is 2.10^{-2}. At each time step, the frame of reference is shifted by a Galilean translation

$$(t, x) \mapsto (t, x + \lambda t). \quad (59)$$

It is expected that u follows this shifting according to (55). Figures 4, left, present, in the original frame of reference, how the standard schemes react to this shifting. They show clearly that, when λ is high, the standard schemes produce locally important errors. In particular, a blow-up arises with the FTCS scheme when $\lambda = 1$. On the contrary, the invariantized version of these schemes present no oscillation, as can be observed on Figures 4, right. Consistency analysis shows that, as the original schemes are no longer consistent with the equation when $\lambda \neq 0$, introducing numerical error, independently of the step sizes. As for them, the invariantized schemes respect the physical property of the equation and provide quasi-identical solutions when λ changes.

Another numerical test was carried out with FTCS scheme. The exact solution is a self-similar solution under projections (54):

$$u(t, x) = \frac{1}{t}\left(x - \tanh(\frac{x}{2\nu})\right). \quad (60)$$

It corresponds to a viscous chock. The chock tends to be entropic when ν becomes closer to 0. Figure 5 show the numerical solutions obtained with the standard and the invariantized FTCS schemes at $t = 2s$, with $\nu = 10^{-2}$, $\Delta t = 5.10^{-2}$ and $\Delta x = 5.10^{-2}$. It shows that the solution given by the invariantized scheme remains close to the exact solution whereas the original FTCS scheme presents a poor performance close to the chock location.

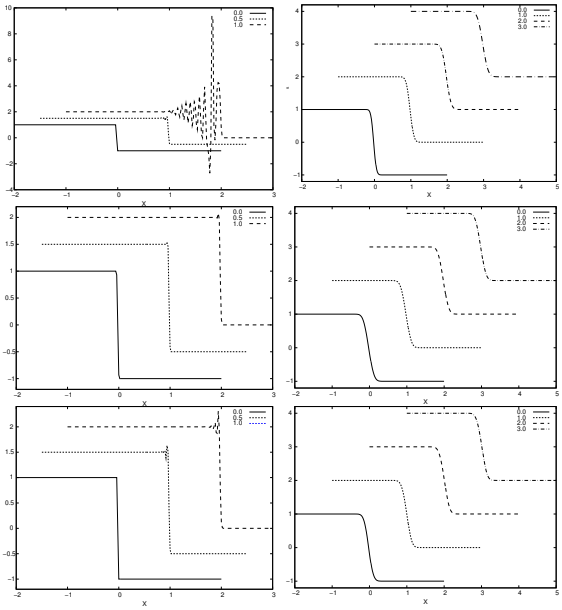

Fig. 4. Approximate solution, with $\lambda = 0, \lambda = 0.5$ and $\lambda = 1$, at $t = 1$s. Left: standard schemes, right: invariantized schemes. Top: FTCS, middle: Lax-Wendroff, bottom: Crank-Nicholson

Since the invariant scheme has the same invariance property as the solution under projections, it does not produce any artificial error. This shows the ability of invariantized scheme to respect the physics of the equation.

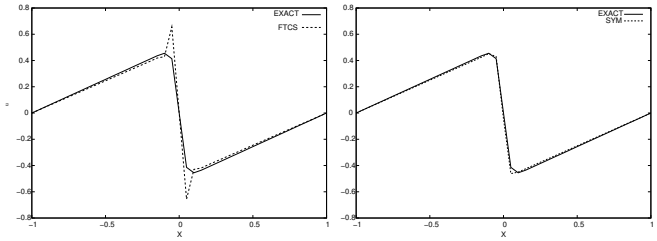

Fig. 5. Numerical solutions with FTCS (left) and invariantized FTCS (right) $\nu = 10^{-2}$. Self-similar case.

VI. Conclusion

Throughout this communication, we showed the importance of Lie-symmetry group theory in engineering science. We also presented ways to preserve symmetries when developing theoretical models and numerical schemes.

References

[1] P. Olver, *Applications of Lie groups to differential equations*, ser. Graduate texts in mathematics. Springer-Verlag, 1986.

[2] N. Ibragimov, *CRC handbook of Lie group analysis of differential equations. Vol 1: Symmetries, exact solutions and conservation laws.* CRC Press, 1994.

[3] N. A. Sayed, A. Hamdouni, E. Liberge, and D. Razafindralandy, "The symmetry group of the non-isothermal navier-stokes equations and turbulence modelling," *Symmetry*, vol. 2, 2010.

[4] B. Cantwell, "Similarity transformations for the two-dimensional, unsteady, stream-function equation," *Journal of Fluid Mechanics*, vol. 85, pp. 257–271, 1978.

[5] E. Nœther, "Invariante Variationsprobleme," in *Königliche Gesellschaft der Wissenschaften*, 1918, pp. 235–257.

[6] D. Razafindralandy, A. Hamdouni, and N. A. Sayed, "Lie-symmetry group and modeling in non-isothermal fluid mechanics," *Physica A: Statistical Mechanics and its Applications*, vol. 391, no. 20, pp. 4624 – 4636, 2012.

[7] M. Oberlack, "A unified approach for symmetries in plane parallel turbulent shear flows," *Proceedings in Applied Mathematics and Mechanics*, vol. 427, pp. 299–328, 2001.

[8] P. Sagaut, *Large eddy simulation for incompressible flows. An introduction. 3rd ed.*, ser. Scientific Computation. Springer, 2006.

[9] D. Razafindralandy and A. Hamdouni, "Invariant subgrid modelling in large-eddy simulation of heat convection turbulence," *Theoretical and Computational Fluid Dynamics*, 2007.

[10] W. Zhang and Q. Chen, "Large eddy simulation of natural and mixed convection airflow indoors with two simple filtered dynamic subgrid scale models," *Numerical Heat Transfer, Part A: Applications*, vol. 37, no. 5, pp. 447–463, 2000.

[11] J. Smagorinsky, "General circulation experiments with the primitive equations," *Monthly Weather Review*, vol. 91, no. 3, pp. 99–164, 1963.

[12] P. Olver, "Geometric foundations of numerical algorithms and symmetry," *Applicable Algebra in Engineering, Communication and Computing*, vol. 11, no. 5, pp. 417–436, 2001.

[13] ——, "Moving frames," *Journal of Symbolic Computation*, vol. 36, no. 3-4, pp. 501–512, 2003.

[14] M. Chhay and A. Hamdouni, "A new construction for invariant numerical schemes using moving frames," *Comptes Rendus Mécanique*, vol. 338, pp. 97–101, 2010.

[15] M. Chhay, E. Hoarau, A. Hamdouni, and P. Sagaut, "Comparison of some lie-symmetry-based integrators," *Journal of Computational Physics*, vol. 230, pp. 2174–2188, 2011.